Cuadernos de Ingeniería. Nueva Serie. Revista de la Facultad de Ingeniería
de la Universidad Católica de Salta (Argentina), núm. 12, 2020

Structure evaluation using output-only systems identification methods and dynamic model updating

Evaluación estructural usando métodos de identificación con base en la respuesta y actualización del modelo dinámico

Andrea Brasiliano[1], Maria Diciá D. Silva[1], Graciela N. Doz[2], José Luís Vital de Brito[2]

Ingeniería Civil / artículo científico

Citar: Brasiliano, A., Silva, M.D., Doz, N. G., & Vital de Brito, J.L. (2020). Structure evaluation using output-only systems identification methods and dynamic model updating. *Cuadernos de Ingeniería*, *12*. Recuperado de http://revistas.ucasal.edu.ar

Recibido: marzo/2020
Aceptado: julio/2020

Abstract
Identifying the dynamic properties of a structure with precision is an important point when trying to establish an adequate methodology for monitoring special structures, since the occurrence of structural damages modifies the original dynamic parameters. In this way, too, it is also possible to calibrate and subsequently work with a robust numerical model as a complement to evaluate structural integrity. Currently, there is no recommended procedure in Brazil to continuously monitor great structures. For this reason, this study aims to work on the proposal of a continuous structural monitoring system for the subsequent evaluation of structural "health". Three identification methods based solely on structural response (Peak Picking, Reference-Based Data-Driven Stochastic Realization and the Reference-Based Covariance-Driven Stochastic Realization) are applied to the results of an experimental test on a three-story frame loaded with different excitation sources. Aspects such as computational effort, precision and processing velocity are analyzed. Subsequently, a method of model updating based on the measured frequencies is also evaluated. The results show that these methods can be an effective part of the intended monitoring methodology.

Key words: system identification, structural evaluation, modal parameters, model update

[1] Departamento de Engenharia Civil e Ambiental, Centro de Tecnologia, Universidade Federal da Paraíba, João Pessoa, Brasil

[2] Departamento de Engenharia Civil e Ambiental, Faculdade de Tecnologia, Universidade de Brasilia, Brasilia, Brasil

Resumen
Identificar las propiedades dinámicas de una estructura con precisión es un punto importante cuando se pretende establecer una metodología adecuada para el monitoreo de obras especiales, ya que la ocurrencia de daños estructurales modifica los parámetros dinámicos originales. De esa forma también, es posible calibrar y trabajar posteriormente con un modelo numérico robusto como complemento para evaluar la integridad estructural. Actualmente, no existe un procedimiento recomendado en Brasil para evaluar continuamente grandes estructuras. Por ese motivo, este estudio tiene como objetivo trabajar en la propuesta de un sistema de monitoreo estructural continuo con vistas a la posterior evaluación de la "salud" estructural. Tres métodos de identificación con base solo en la respuesta estructural (Peak Picking, Reference-Based Data-Driven Stochastic Realization and the Reference-Based Covariance-Driven Stochastic Realization) son aplicados a los resultados de un ensayo experimental de un pórtico de tres pisos sometido a diferentes fuentes de excitación. Son analizados aspectos como el esfuerzo computacional, la precisión y la velocidad de procesamiento. Posteriormente se evalúa también un método de actualización del modelo numérico basado en las frecuencias medidas. Los resultados muestran que estos métodos pueden constituir una parte efectiva de la metodología de monitoreo pretendida..

Palabras clave: identificación de sistemas, evaluación estructural, parámetros modales, actualización del modelo numérico.

1. Introduction

In general, structures must support permanent loads or environmental excitations, such as wind, traffic, earthquakes and impacts. Over the years, these structures may deteriorate under normal conditions of use. Not only can this affect its load capacity, but excessive cracks may form, producing vibrations which induce discomfort and insecurity for their users.

A reliable structure evaluation is necessary to detect the existence and location of structural damages in order to establish maintenance and repair procedures that will improve overall structural integrity. Doebling *et al*. (1998) and Zou *et al*. (2000) explain that the dynamic properties may be used for damage detection, since the occurrence of failures modifies the natural frequencies of the structure, and the modal shapes enable the location of possible damages. Thus, the use of efficient system identification methods is significant for a better structural evaluation, obtaining accurate results with minimum errors.

Great structures such as bridges, footbridges, stadiums and overpasses, are affected by environmental excitation. This kind of excitation cannot be easily measured because of its stochastic behavior, so the use of output-only system identification methods is necessary. For these methods, the input data are not needed to identify the dynamic properties of the structure, but only the output data such as acceleration records are required. Peeters and De Roeck (1999) and Peeters (2000) presented important studies about time domain output-only methods. In those works, the authors made improvements on the SSI-DATA and SSI-COV methods by considering only some of the structure's response as reference outputs in order to identify the modal parameters. The methods studied by the authors correspond to stochastic ones and in this case the excitation is modeled by terms of white-noise. This present work shows that the stochastic methods allow the identification of the modal parameters even though the excitations applied were not a white-noise.

On the other hand, having a robust numerical model is also essential for monitoring structural systems. With a numerical model updated with the dynamic characteristics experimentally identified, for example, it is possible to obtain more realistic results: it will be guaranteed that the model represents the behavior of the real structure as close as possible. The output-only system identification that obtains the dynamic properties of a structure is not able to identify its unknown parameters, such as physical and/or geometric properties. However, these parameters may be determined (or updated) by finite element model updating based on the dynamic characteristics identified experimentally. In general, the finite element model updating in structural dynamics is used to adjust numerical models to the experimental results by means of direct or iterative methods. Model updating using iterative methods based on dynamic characteristics provides the determination of unknown parameters such as stiffness, mass, or damping. Thus, it can be used as an important tool for evaluation of the behavior or condition of the structures. Brownjohn *et al*. (2001) described a finite element model updating method based on sensitivity analysis and its application on the evaluation of structural conditions. The authors also investigated the efficiency of the method in damage quantification.

The updated numerical model of a structure, from the measured data, such as frequencies and mode shapes, can be used as precise tool to foresee its dynamic behavior due to modifications suffered during its useful life. The monitoring of great structures is not considered to be as important as it should be in Brazil. This is evident from recent accidents with some overpasses caused by the lack of maintenance. In 2018, two structures collapsed under normal conditions of use. In Brasília (Federal District), an important overpass failed because of an undetected infiltration that caused a considerable deterioration of the structure leading it to the rupture (Carone, 2018). Later, in São Paulo another overpass subjected to a heavy traffic presented deterioration on its support which caused the fall of a part of the structure (Cerqueira, 2018).

In this sense, searching to establish a suitable methodology for the structure evaluation, this work presents an experimental study in which output-only system identification methods, in the time and frequency domains, and a numerical model update method based on penalty functions were applied and evaluated. The analyzed structure was a simple metallic frame with three degrees of freedom. The frame was submitted to vibration tests in which different types of excitations were applied. The Peak Picking, the Reference-Based Data-Driven Stochastic Realization (SSI-DATA/ref) and the Reference-Based Covariance-Driven Stochastic Realization (SSI-COV/ref) methods were applied in order to identify the natural frequencies and the mode shapes of the frame. The influence of excitation source in the identification of the modal parameters was also evaluated.

The choice of the mentioned methods considered some aspects. The Peak Picking method, for example, was chosen because of its simplicity, relative facility of implementation and also the fact that once it works at frequency domain, it would be faster to identify the natural frequencies observing the peaks of the signal spectrum. On the other hand, Peeters (2000) showed that this method provides better results when the structures present a spectrum with well separated natural frequencies. The identification of the respective natural mode shapes is not so simple because in some cases it could require a manual procedure to search for the correct peaks that will form the mode shapes. The stochastic subspace methods (SSI-DATA/ref and SSI-COV/ref) only require the output signals of the structure to provide its dynamic properties and work in time-domain; they were also chosen for their robustness and precision, as demonstrated by Peeters (2000).

The finite element model of the frame was updated by the Penalty Function Method (Friswell and Mottershead, 1995) using the measured frequencies. It is an iterative method which permits the obtainment of updated parameters with physical meaning: it is believed that it can be used as a tool to evaluate structural conditions.

The results showed that the applied tools had a good overall performance, indicating that their choice would be succeed for the purpose of monitoring structural systems.

2. Peak Picking Method

According to Peeters (2000), the Peak Picking Method (PPM) is a classical technique and the simplest one to estimate modal parameters of structures under ambient vibration. This method works in frequency domain and has a great application in Civil Engineering, because of its simplicity and processing time. However, better results are found for structures that have well separated natural frequencies and low damping conditions.

The Peak Picking Method applies the Discrete Fourier Transform to the output data in the time domain to transform it to the frequency domain. Then, it obtains the Power Spectral Density Function (PSD) of the system output. To optimize the PSD acquisition, the Modified Welch Periodogram (Welch, 1967) is a computational alternative that divides the signal in segments and applies the *Hanning* window that removes any signal discontinuity. The natural frequencies of the structure are estimated by the peaks of the acquired output spectral density.

The modal configuration has the same direction as the one chosen for the sensors used in the test. The relation between the peak magnitude of each sensor and that related to the reference one indicates the modal amplitudes. For a mode i, the modal amplitude of each measured point j will be defined as follows:

$$A_{i,j} = \sqrt{\frac{\mathrm{PSD}_{ij}}{\mathrm{PSD}_{iref}}} \tag{1}$$

where PSD_{ij} represents the peak of the spectral density that corresponds to mode i at point j and PSD_{iref} represents the peak of the spectral density that corresponds to mode i at reference point.

The signal of the modal amplitude is determined by the cross-spectral density function between the outputs of all sensors and the reference one. According to Palazzo (2001), the positive or negative signal will be defined from the phase of this cross-spectral density function according to the following ranges: if $-70^o < \varphi < 70^o$, the amplitude will be positive; if $-250^o < \varphi < -110^o$ or $110^o < \varphi < 250^o$, the amplitude will be negative.

3. Reference-Based Data-Driven Stochastic Realization (SSI-DATA/ref)

The Reference-Based Data-Driven Stochastic Realization (SSI-DATA/ref) is a reformulation of the Data-Driven Stochastic Subspace Identification (SSI-DATA) (Peeters and De Roeck, 1999). This method identifies a stochastic state space model (Eq. 2) directly from the time records for a white noise excitation.

$$\boldsymbol{x}_{k+1} = \boldsymbol{A}x_k + \boldsymbol{\varpi}_k;\ \boldsymbol{y}_k = \boldsymbol{C}\boldsymbol{x}_k + \boldsymbol{v}_k \tag{2}$$

where matrices **A** and **C** describe the relation between the input and the output vector, $\boldsymbol{y}_k$, of a system by a discrete time state vector $\boldsymbol{x}_k$; $\boldsymbol{\varpi}_k \in \boldsymbol{R}^{n\ x\ 1}$ is the process noise due to disturbances and modeling inaccuracies and $\boldsymbol{v}_k \in \boldsymbol{R}^{l\ x\ 1}$ is the measurement noise due to sensor inaccuracies. Consider k the index related to the response of the structure obtained in discrete time intervals, n is the system order identified by the method and l is the number of measuring points.

In an experimental test, the position and the number of sensors help to determine the mode shapes of a structure. All signals acquired by the sensors carry the same information about the modal properties, if none of them is placed at a node of a mode and it means that measures typically contain some redundancy. To improve the processing time and decrease this redundancy without losing accuracy, some signals may be partially omitted in the identification process and at the end, they are again included in order to obtain the "full" mode shapes. Assume that the l outputs are split in a subset of r well-chosen reference sensors and a subset of $l-r$ other sensors. Some identification methods use the block Hankel matrix (Eq. 3) composed by *2i* block rows and N columns to gather the output measurements.

$$\boldsymbol{H}^{\mathrm{ref}} \equiv \frac{1}{\sqrt{N}} \left[\begin{array}{cccc} \boldsymbol{y}_0^{\mathrm{ref}} & \boldsymbol{y}_1^{\mathrm{ref}} & \cdots & \boldsymbol{y}_{N-1}^{\mathrm{ref}} \\ \boldsymbol{y}_1^{\mathrm{ref}} & \boldsymbol{y}_2^{\mathrm{ref}} & \cdots & \boldsymbol{y}_N^{\mathrm{ref}} \\ \vdots & \vdots & \cdots & \vdots \\ \boldsymbol{y}_{\mathrm{i-1}}^{\mathrm{ref}} & \boldsymbol{y}_i^{\mathrm{ref}} & \cdots & \boldsymbol{y}_{i+\mathrm{N-2}}^{\mathrm{ref}} \\ \hline \boldsymbol{y}_i & \boldsymbol{y}_{i+1} & \cdots & \boldsymbol{y}_{i+\mathrm{N-1}} \\ \boldsymbol{y}_{i+1} & \boldsymbol{y}_{i+2} & \cdots & \boldsymbol{y}_{i+N} \\ \vdots & \vdots & \cdots & \vdots \\ \boldsymbol{y}_{\mathrm{2i-1}} & \boldsymbol{y}_{\mathrm{2i}} & \cdots & \boldsymbol{y}_{\mathrm{2i}+N-2} \end{array}\right] \equiv \left[\frac{\boldsymbol{Y}_{0|i-1}^{\mathrm{ref}}}{\boldsymbol{Y}_{i|\mathrm{2i}-1}}\right] \equiv \left[\frac{\boldsymbol{Y}_p^{\mathrm{ref}}}{\boldsymbol{Y}_f}\right] \begin{array}{l} \updownarrow \mathrm{ri}\ \text{"past"} \\ \updownarrow \mathrm{li}\ \text{"future"} \end{array} \in \boldsymbol{R}^{(r+l)\ \mathrm{i\ x}\ N} \tag{3}$$

where $\boldsymbol{y}_k^{\mathrm{ref}} \in \boldsymbol{R}^{r\ \mathrm{x}\ 1}$ are the reference outputs and $\boldsymbol{y}_k \in \boldsymbol{R}^{l\ \mathrm{x}\ 1}$ are the others and i is the time lag. The terms *past* and *future* refer to the time instants in which the outputs were obtained. It means that the subset of all future outputs was obtained at time instants posterior to that corresponding to the reference outputs.

According to Peeters (2000) and Brasiliano (2005) and based on the concepts of Kalman Filter (Juang, 1994; Chen, 1999) a projection matrix $\boldsymbol{P}_{\boldsymbol{i}}^{\mathbf{ref}}$ can be obtained from *QR decomposition* of the Hankel matrix. Then, the observability matrix $\boldsymbol{O}_{\boldsymbol{i}}$ and the Kalman filter state sequence $\widehat{\boldsymbol{X}}_{i}$ can be obtained by applying singular value decomposition (SVD) to the projection matrix $\boldsymbol{P}_{\boldsymbol{i}}^{\mathbf{ref}}$ (Eq. 4):

$$\boldsymbol{P}_{\boldsymbol{i}}^{\mathbf{ref}} = \boldsymbol{U}_{\mathbf{1}}\boldsymbol{S}_{\mathbf{1}}\boldsymbol{V}_{\mathbf{1}}^{\boldsymbol{T}} \Rightarrow \boldsymbol{O}_{\boldsymbol{i}} = \boldsymbol{U}_{\mathbf{1}}\boldsymbol{S}_{\mathbf{1}}^{\mathbf{1/2}} \Rightarrow \widehat{\boldsymbol{X}}_{i} = \boldsymbol{O}_{i}^{*}\boldsymbol{P}_{i}^{\mathrm{ref}} \tag{4}$$

where $\boldsymbol{O}_{i}^{*}$ represents the pseudo-inverse of observability matrix.
The extended observability matrix $\boldsymbol{O}_{\mathrm{i\text{-}1}}$ can be simply obtained after deleting the last l rows of $\boldsymbol{O}_{\boldsymbol{i}}$ and $\boldsymbol{P}_{\mathrm{i\text{-}1}}^{\mathrm{ref}} \in \boldsymbol{R}^{l(\mathrm{i\text{-}1})\ \mathrm{x}\ N}$ can be defined and also be represented by submatrices $\boldsymbol{R}_{41}$, $\boldsymbol{R}_{42}$, $\boldsymbol{Q}_{1}^{T}$ and $\boldsymbol{Q}_{2}^{T}$ obtained from the *QR decomposition* of the Hankel matrix (Brasiliano, 2005) (Eq. 5).

$$\boldsymbol{P}_{\mathrm{i\text{-}1}}^{\mathrm{ref}} = \frac{\boldsymbol{Y}_{f}^{-}}{\boldsymbol{Y}_{P}^{\mathrm{ref}+}} = \boldsymbol{O}_{\mathrm{i\text{-}1}}\widehat{\boldsymbol{X}}_{\mathrm{i\text{-}1}};\ \boldsymbol{P}_{\mathrm{i\text{-}1}}^{\mathrm{ref}} = [\boldsymbol{R}_{41} \quad \boldsymbol{R}_{42}]\begin{bmatrix}\boldsymbol{Q}_{1}^{T}\\ \boldsymbol{Q}_{2}^{T}\end{bmatrix} \tag{5}$$

The system matrices can be determined by solving the following linear system equation for **A** and **C** in a least square sense (Eq. 6):

$$\begin{bmatrix}\boldsymbol{A}\\ \boldsymbol{C}\end{bmatrix} = \begin{bmatrix}\widehat{\boldsymbol{X}}_{\mathrm{i\text{-}1}}\\ \boldsymbol{Y}_{i|i}\end{bmatrix}\widehat{\boldsymbol{X}}_{i}^{\ *}; \qquad \boldsymbol{Y}_{i|i} = \begin{bmatrix}\boldsymbol{R}_{21} & \boldsymbol{R}_{22} & \mathbf{0}\\ \boldsymbol{R}_{31} & \boldsymbol{R}_{32} & \boldsymbol{R}_{33}\end{bmatrix}\begin{bmatrix}\boldsymbol{Q}_{1}^{T}\\ \boldsymbol{Q}_{2}^{T}\\ \boldsymbol{Q}_{3}^{T}\end{bmatrix} \tag{6}$$

In which $\boldsymbol{Y}_{i|i}$ is a Hankel matrix with only one block row, and $\widehat{\boldsymbol{X}}_{i}^{\ *}$ represents the pseudo-inverse matrix of $\widehat{\boldsymbol{X}}_{i}$ defined in Eq. (4).

The discrete state matrix **A** and the observation matrix **C** solve the identification problem. Rahman (2012) and Schanke (2015) explain how to obtain the dynamic properties from these matrices. The dynamic behavior of the system is characterized by the eigenvalues and eigenvectors of continuous matrix **A**.

The eigenvalues of continuous state matrix **A** are obtained from the relation between the continuous and discrete systems (Eq. 7). Considering the continuous eigenvalues, the natural frequencies correspond to the imaginary part of them (Eq. 8) and the mode shapes are obtained by the product of the eigenvectors of matrix **A** and the observation matrix **C**.

$$\lambda = \frac{ln(\mu)}{\Delta t} \tag{7}$$

$$f = \frac{Im(\lambda)}{2\pi} \tag{8}$$

where λ are the eigenvalues of continuous state matrix **A**; μ are the eigenvalues of discrete state matrix **A**; Δt is the time interval between the measured records and f is the natural frequencies of the damped system, in *Hertz*.

Peeters and De Roeck (2001) also suggest the use of a stabilization diagram to the application of the SSI-DATA method. The order of the system is overestimated because of noises that may occur in the experimental data acquisition; it also creates nonphysical and mathematical poles next to the physical poles.

The purpose of the stabilization diagram is to separate the physical poles, which are stable, from the mathematical poles, which are not stable. The pole is stable when the differences between natural frequencies, damping ratios, and mode shapes are within the stabilization criteria defined by the user. The stable pole alignment identifies the natural frequencies of the vibration modes (Peeters and De Roeck, 2001; Schanke, 2015).

According to Shancke (2015), it is necessary to estimate an appropriated value for the maximal order (n_{max}). If the maximal order is smaller than the correct system order, incorrect results will be obtained. If the chosen value is too high then a lot of nonphysical poles will appear, making it difficult to find the correct results and increasing the computational time. The data matrix should be $l \; x \; N$, where l is the number of measurement channels and N is the number of measurements. The magnitude of block rows, b, is chosen by the user.

4. Reference-Based Covariance-Driven Stochastic Realization

The Reference-Based Covariance-Driven Stochastic Realization (SSI-COV/ref) is a reformulation of the Covariance-Driven Stochastic Subspace Identification (SSI-COV), both developed by Peeters and De Roeck (1999). The method identifies a stochastic state-space model using the output covariance matrices between all outputs and the reference ones, assuming a white noise excitation.

Considering the output-only data obtained from experimental tests, Eq. (9) calculates the covariances between all outputs and the reference ones:

$$\boldsymbol{R}_i^{ref} \equiv E\left[\boldsymbol{y}_{k+i}\boldsymbol{y}_k^{ref^T}\right] \in \boldsymbol{R}^{l\times r} \tag{9}$$

where l is the number of outputs, r is the number of reference sensors and i is the time lag.

Considering that a finite number N of data is available and the important factorization property of stochastic systems $\boldsymbol{R}_i^{\mathrm{ref}} = \boldsymbol{R}_i\boldsymbol{L}_l^T = \boldsymbol{C}\boldsymbol{A}^{i-1}\boldsymbol{G}^{ref}$, where $\boldsymbol{G}^{ref}$ is the *next-state output covariance* *matrix,* the output covariances R_i^{ref} may be gathered in a block Toeplitz matrix $\boldsymbol{T}_{1|i}^{\mathrm{ref}} \in \boldsymbol{R}^{li \times ri}$ (Eq. 10) that can be computed from the data block Hankel matrix (Eq. 3) defined previously. The *next-state output covariance matrix* G^{ref} correspond to the last columns of controllability matrix C_i^{ref} (Brasiliano, 2005). Then, the application of the *Singular Value Decomposition* (SVD) to the Toeplitz matrix (Eq. 11) allows the estimation of its rank, n, as the number of singular values other than zero.

$$\boldsymbol{T}_{1|i}^{\mathrm{ref}} = \boldsymbol{Y}_f \boldsymbol{Y}_p^{\mathrm{ref}\,T} = \begin{bmatrix} \boldsymbol{R}_i^{\mathrm{ref}} & \boldsymbol{R}_{\mathrm{i\text{-}1}}^{\mathrm{ref}} & \cdots & \boldsymbol{R}_1^{\mathrm{ref}} \\ \boldsymbol{R}_{i+1}^{\mathrm{ref}} & \boldsymbol{R}_i^{\mathrm{ref}} & \cdots & \boldsymbol{R}_2^{\mathrm{ref}} \\ \vdots & \vdots & \vdots & \vdots \\ \boldsymbol{R}_{\mathrm{2i\text{-}1}}^{\mathrm{ref}} & \boldsymbol{R}_{\mathrm{2i\text{-}2}}^{\mathrm{ref}} & \cdots & \boldsymbol{R}_i^{\mathrm{ref}} \end{bmatrix} =$$

$$= \underbrace{\begin{bmatrix} \boldsymbol{C} \\ \boldsymbol{CA} \\ \boldsymbol{CA}^2 \\ \vdots \\ \boldsymbol{CA}^{i-1} \end{bmatrix}}_{\overleftrightarrow{n}} \left[\boldsymbol{A}^{i-1}\boldsymbol{G}^{ref} \quad \boldsymbol{A}^{i-2}\boldsymbol{G}^{ref} \quad \cdots \quad \boldsymbol{AG}^{ref}\right] \updownarrow n = \boldsymbol{O}_i \boldsymbol{C}_i^{ref} \tag{10}$$

$$\boldsymbol{T}_{1|i}^{ref} = \boldsymbol{USV}^T = [\boldsymbol{U}_1 \quad \boldsymbol{U}_2] \begin{bmatrix} \boldsymbol{S}_1 & 0 \\ 0 & 0 \end{bmatrix} \begin{bmatrix} \boldsymbol{V}_1^T \\ \boldsymbol{V}_2^T \end{bmatrix} = \boldsymbol{U}_1 \boldsymbol{S}_1 \boldsymbol{V}_1^T \tag{11}$$

where $\overleftrightarrow{n}$ and $\updownarrow n$ are mathematical operators that indicate the number n of columns and rows, $\boldsymbol{U} \in R^{li \times li}$ and $\boldsymbol{V} \in R^{ri \times ri}$ are orthonormal matrices and $\boldsymbol{S} \in R^{li \times ri}$ is a diagonal matrix whose elements are the positive singular values in descending order. Splitting the SVD in two parts, the extended observability matrix $\boldsymbol{O}_i \in \boldsymbol{R}^{li \times n}$ and extend stochastic controllability matrix $\boldsymbol{C}_i^{\mathrm{ref}} \in \boldsymbol{R}^{n \times ri}$ (Eq. 12) are computed and the identification problem may be solved.

$$\boldsymbol{O}_i = \boldsymbol{U}_1 \boldsymbol{S}_1^{\frac{1}{2}}; \ \boldsymbol{C}_i^{ref} = \boldsymbol{S}_1{}^{1/2} \boldsymbol{V}_1^T \tag{12}$$

From Eq. 12, is possible to obtain the state matrix **A**, the next-state output covariance matrix $\boldsymbol{G}^{\mathrm{ref}}$ and the observation matrix **C**. The matrix **A** can be obtained by the decomposition property of a shifted block Toeplitz matrix $\mathbf{T}_{2|i+1}^{\mathrm{ref}}$ which is composed of covariances $\mathbf{R}_{\mathrm{k}}^{\mathrm{ref}}$ from time lag

2 to $i+1$ but has a similar structure as $\mathbf{T}_{1|i}^{\text{ref}}$. As described in the SSI-DATA/ref method, the modal parameters may be computed from matrices **A** and **C** and the stabilization diagram can also be applied.

5. Finite element model updating by the Penalty Function Method (Friswell & Mottershead, 1995)

The purpose of dynamic model updating is modifying parameters of the numerical model in order to improve the correlation between the measured data and the results from the analytical model. The model updating can be done using direct or iterative methods. The iterative methods obtain parameters with physical meaning and they can be used as a tool to evaluate structural conditions. Because of this, an iterative method based on penalty functions was applied in this paper.

According to Friswell & Mottershead (1995), the penalty functions are generally non-linear functions of the parameters, and the iterative procedure is required with the possible associated convergence problems. Thus, the penalty function determines the correlation involving the mode shape and eigenvalue data and normally uses a truncated Taylor series expansion of the modal data in terms of the unknown parameters (Eq. 13).

$$\delta z = \boldsymbol{S}_j \delta \boldsymbol{\theta} \tag{13}$$

where $\boldsymbol{\delta\theta} = \boldsymbol{\theta} - \boldsymbol{\theta}_j$ is the perturbation in the parameters; $\delta \boldsymbol{z} = \boldsymbol{z}_m - \boldsymbol{z}_j$ is the difference between the measured and the estimated eigenvalue $\boldsymbol{z}_m$ and $\boldsymbol{z}_{j,}$ respectively, and $\boldsymbol{S}_j$ is the sensitivity matrix. In Eq. (13) $\boldsymbol{\theta}_j$ is the current parameter estimate after j iterations and m indicates the number of measured points. The sensitivity matrix can be obtained by several methods such as that proposed by Fox & Kapoor (1968) where the first derivative of the eigenvalues is computed as follows (Eq. 14):

$$\frac{\delta \lambda_i}{\delta \boldsymbol{\theta}} = \varphi_i^T \left[\frac{\delta \boldsymbol{K}}{\delta \boldsymbol{\theta}} - \lambda_i \frac{\delta \boldsymbol{M}}{\delta \boldsymbol{\theta}} \right] \varphi_i \tag{14}$$

where φ_i is the eigenvector corresponding to λ_i, $\frac{\delta \boldsymbol{K}}{\delta \boldsymbol{\theta}}$ and $\frac{\delta \boldsymbol{M}}{\delta \boldsymbol{\theta}}$ are matrices obtained by the derivative of each element of the system stiffness matrix $\boldsymbol{K}$ and the system mass matrix $\boldsymbol{M}$, respectively, according to the parameters that are being updated.

In practice, the number of unknown parameters frequently will exceed the number of measured data. In these cases, the problem consists of minimizing the following penalty function (Eq. 15):

$$J(\delta\boldsymbol{\theta}) = \delta\boldsymbol{z}^T\boldsymbol{W}_{\varepsilon\varepsilon}\delta\boldsymbol{z} + (\boldsymbol{\theta}_j - \boldsymbol{\theta}_0)^T\boldsymbol{W}_{\theta\theta}(\boldsymbol{\theta}_j - \boldsymbol{\theta}_0) - 2\delta\boldsymbol{\theta}^T\{\boldsymbol{S}^T\boldsymbol{W}_{\varepsilon\varepsilon}\delta\boldsymbol{z} - \boldsymbol{W}_{\theta\theta}(\boldsymbol{\theta}_j - \boldsymbol{\theta}_0)\} + \delta\boldsymbol{\theta}^T[\boldsymbol{S}^T\boldsymbol{W}_{\varepsilon\varepsilon}\boldsymbol{S} + \boldsymbol{W}_{\theta\theta}]\delta\boldsymbol{\theta} \tag{15}$$

where $\boldsymbol{\theta}_0$ is the vector of the estimated initial parameters, $\boldsymbol{W}_{\varepsilon\varepsilon}$ is a diagonal matrix whose elements are equal to the inverse of the variance of the corresponding eigenvalues. The matrix $\boldsymbol{W}_{\theta\theta}$ is also a weighting matrix and its elements are the inverse of the estimated variance of the corresponding parameters.

Minimizing this function with respect to $\delta\boldsymbol{\theta}$, one obtains (Eq. 16):

$$\boldsymbol{\theta}_{j+1} = \boldsymbol{\theta}_j + \left(\mathbf{S}_j^T\mathbf{W}_{\boldsymbol{\varepsilon\varepsilon}}\mathbf{S}_j + \mathbf{W}_{\boldsymbol{\theta\theta}}\right)^{-1}\left\{\mathbf{S}_j^T\mathbf{W}_{\boldsymbol{\varepsilon\varepsilon}}(\mathbf{z}_m - \mathbf{z}_j) - \mathbf{W}_{\boldsymbol{\theta\theta}}(\boldsymbol{\theta}_j - \boldsymbol{\theta}_0)\right\} \tag{16}$$

The weighting matrix $\boldsymbol{W}_{\theta\theta}$ must be positive definite and is chosen so that parameters which are estimated accurately in the initial finite element model do not change as much as parameters whose initial estimates are poor. $\boldsymbol{W}_{\theta\theta}$ is also a diagonal matrix whose elements are the reciprocals of the estimated variances (the squares of the standard deviations) of the corresponding parameters. Despite the variance may be difficult to estimate quantitatively, the ability to set level of uncertainty in the parameters is very powerful. The choice of these matrices, $\boldsymbol{W}_{\varepsilon\varepsilon}$ and $\boldsymbol{W}_{\theta\theta}$, which allow the attribution of relative uncertainty in the parameters and measurements (eigenvalues) is based on the estimated standard deviations. According to Friswell and Mottershead (1995), an important feature in using penalty function methods is that the absolute value of the weighting matrices is of no consequence.

6. Experimental Analysis

This section will present the results obtained from the application of systems identification and model updating methods to experimental data. In the experimental analysis, vibration tests in a three-story shear frame (shear building model) were realized and the identification methods of dynamic properties (SSI-COV/ref, SSI-DATA/ref and the Peak Picking Method) was applied to the acceleration records obtained from the tested structure. Vibration tests considering three different types of excitation applied in different points were realized. With respect to the updating of the numerical frame model, the method based on penalty function and sensitivity analysis (Friswell and Mottershead, 1995) was applied.

6.1 Characteristics of the frame and vibration tests

The frame was built with four aluminum bars and two steel rules. The steel rules were fixed to the aluminum bars by screws, as can be seen in Fig. 1. The values of the frame components masses are summarized in Table 1. There was also an electric motor fixed at the second floor.

Fig. 1 presents a scheme of the frame as well its dimensions and coordinates.

Table 1. Masses of the frame components.

	Mass (kg)
Bar 1	0.28063
Bar 2	0.15938
Bar 3	0.15903
Bar 4	0.15892
Rule 1	0.10503
Rule 2	0.10469
Electric Motor	0.15300
Accelerometer	0.02814

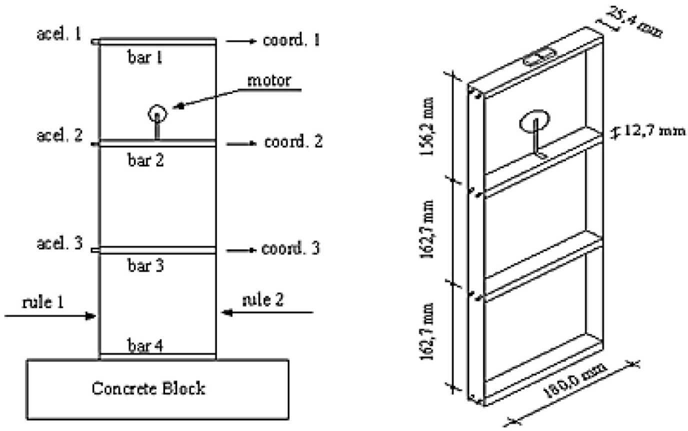

Fig. 1. Configuration of the tested frame.

For calculating the mass matrix, the masses of all frame elements showed in Table 1 were considered. The frame's stiffness matrix was built considering a shear building model once the bars' stiffness could be considered infinite compared to the rules' stiffness. According to Clough and Penzien (1993), the system identification methods work for shear building structures such as regular frames, the difference is that only the lower stiffness elements need to be considered in the methods, which improves the computational processing. As can be seen in Fig. 1, the bars represent the floors and the rules represent the columns of the experimental model. The mass and stiffness matrices were defined as follows (Eq. 17):

$$\mathbf{M}=\begin{bmatrix}0{,}3500402 & 0 & 0\\ 0 & 0{,}4196357 & 0\\ 0 & 0 & 0{,}2677009\end{bmatrix}\text{kg};\;\; \mathbf{K}=\begin{bmatrix}24EI/l_1^3 & -24EI/l_1^3 & 0\\ -24EI/l_1^3 & \left(24EI/l_1^3+24EI/l_2^3\right) & -24EI/l_2^3\\ 0 & -24EI/l_2^3 & \left(24EI/l_2^3+24EI/l_3^3\right)\end{bmatrix}\text{N/m} \tag{17}$$

The Young's Modulus (E) and inertia moment (I) of the frame column were considered as: $E = 2.06 \times 10^{11}\ N/m^2$; $I = 3.219 \times 10^{-12}\ m^4$. The frame was fixed in a concrete block with 50kg in weight and the block was put on a rubber plate in order to avoid base vibration. Three piezoelectric accelerometers with sensitivity equal to $4{,}80\, pC/ms^{-2}$ were fixed to the three coordinates of the frame (Fig. 1).

The frame was submitted to the following tests: two free vibration tests and one forced vibration, named Test 1, Test 2, and Test 3. Tests 1 and 2 correspond to the free vibration tests produced by an impact at coordinate 1 (third floor) of the frame and by an initial displacement at this point, respectively. Test 3 corresponds to the forced vibration test produced by an electric motor fixed at the second floor of the frame. The acquisition equipment was configured to acquire the records with a sample time of 5×10^{-3}s resulting in a sample frequency of 200 Hz $(1/\Delta t)$. The records were acquired during 25s.

Since the identification methods applied are output-only methods, they do not require information from the excitation sources, just the output signals (accelerations records, for example) are necessary to the identification of the dynamic properties and therefore no measure of the excitations has been considered. It is important to emphasize that the excitations have been applied observing the sensitivity of the used accelerometers in order to provide reliable acceleration records. Numerical simulations were performed by Brasiliano (2005) to validate the implemented computational algorithms.

6.2 Identification of the dynamic properties of the frame

The natural frequencies and mode shapes of the structure were identified from the acceleration records that were acquired in the vibration tests. This identification was done by the three methods already cited. Fig. 2 presents the acceleration records obtained from the accelerometer 1 in Fig. 1. The power spectral functions used in the Peak Picking Method, for tests 1, 2, and 3 are shown in Fig. 3.

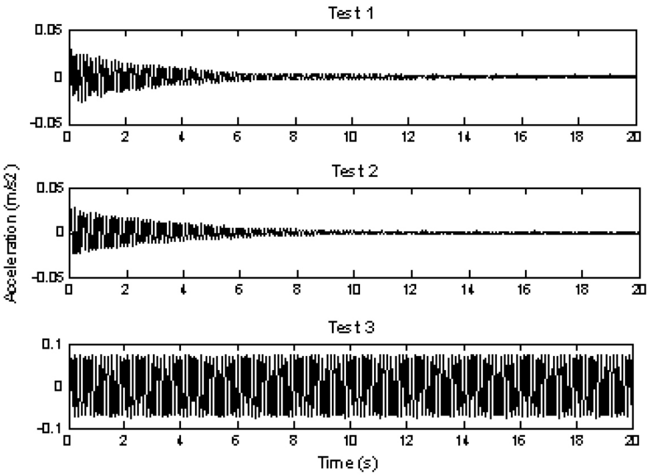

Fig. 2. Acceleration records from the coordinate 1.

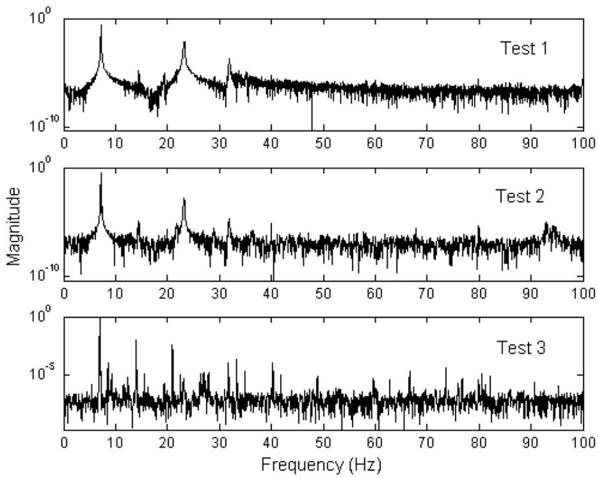

Fig. 3. Power spectral density of the acceleration records obtained at coordinate 1.

The Peak Picking Method enables the identification of the peaks which correspond to the natural frequencies in the PSD functions (Fig 3) for tests 1 and 2. However, for test 3 the peaks are not well defined; this is most likely due to the presence of frequencies of the electric motor, which required a manual analysis of the results. Following this analysis, and consideration of the theoretical values obtained, it was possible to identify the natural frequencies of the frame for test 3. The theoretical results correspond to those obtained from the solution of the eigenvalue problem (Eq. 18).

$$\boldsymbol{K}\,\boldsymbol{\Phi} - (\boldsymbol{M}\,\boldsymbol{\Phi})\boldsymbol{\Lambda} = \mathbf{0} \tag{18}$$

where **K** and **M** are the structure stiffness and mass matrices, respectively, $\boldsymbol{\Phi}$ is the matrix which columns are the mode shapes and $\boldsymbol{\Lambda}$ is a diagonal matrix which elements are the eigenvalues.

The frequencies, including their percentage difference relative to the theoretical frequencies, and the mode shapes identified by each method are presented in Table 2 and Figs. 4a to 4c, respectively.

About the results of the mode shapes, when the impact or the initial displacement was applied to coordinate 1 of the frame, tests 1 and 2, the three mode shapes can be identified by all methods correctly (Fig 4a and 4b).

Table 2. Natural frequencies identified by the methods.

				Test 1			
Mode Shapes	Theoretical Frequency (Hz)	Peak Picking		SSI-COV/ref		SSI-DATA/ref	
		Frequency (Hz)	Difference (%)	Frequency (Hz)	Difference (%)	Frequency (Hz)	Difference (%)
1st	7.158	7.220	0.866	7.231	1.020	7.230	1.006
2nd	22.219	23.220	4.505	23.207	4.447	23.183	4.339
3rd	30.524	31.902	4.514	31.869	4.406	31.868	4.403
				Test 2			
Mode Shapes	Theoretical Frequency (Hz)	Peak Picking		SSI-COV/ref		SSI-DATA/ref	
		Frequency (Hz)	Difference (%)	Frequency (Hz)	Difference (%)	Frequency (Hz)	Difference (%)
1st	7.158	7.220	0.866	7.225	0.936	7.222	0.894
2nd	22.219	23.220	4.505	23.181	4.330	23.179	4.321
3rd	30.524	31.805	4.197	31.861	4.380	31.859	4.374
				Test 3			
Mode Shapes	Theoretical Frequency (Hz)	Peak Picking		SSI-COV/ref		SSI-DATA/ref	
		Frequency (Hz)	Difference (%)	Frequency (Hz)	Difference (%)	Frequency (Hz)	Difference (%)
1st	7.158	6.927	-3.227	7.666	7.097	6.983	-2.445
2nd	22.219	20.878	-6.035	20.989	-5.536	21.176	-4.694
3rd	30.524	31.707	3.876	32.924	7.863	32.730	7.227

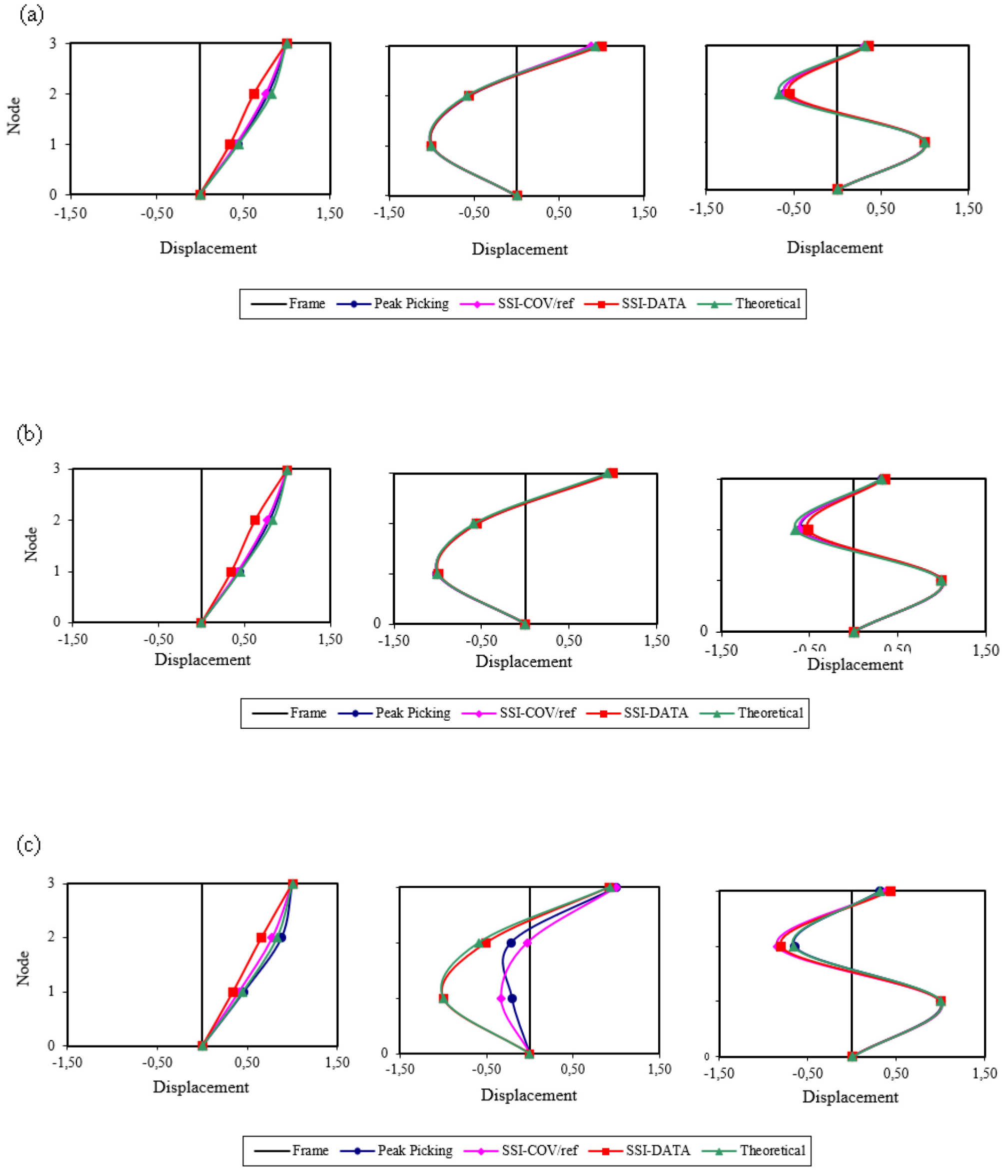

Fig. 4. Mode shapes identified by the methods. (a) Test 1; (b) Test 2 and (c) Test 3.

The forced vibration test (Test 3) verified the three mode shapes were identified by all methods, but only the SSI-DATA/ref had a better matching with the theoretical mode shapes. The mode shapes identified by Peak Picking Method and the SSI-COV/ref presented different amplitudes, as shown in Fig 4c. With respect to the frequencies, the values presented in Table 2 indicate that all methods have identified this modal property correctly.

The stochastic system identification methods (SSI-DATA/ref; SSI-COV/ref) consider the hypothesis that the input or excitation can be represented by a white noise. However, despite this hypothesis had been violated, in Test 3, when the described type of excitation was applied to the frame, the dynamic properties of the structure were identified satisfactorily.

Fig. 5 and 6 present the stabilization diagram obtained by SSI-COV and SSI-DATA methods for all tests. The stabilization criteria are 0.5% for natural frequencies and 5% for damping ratios. For both methods, the maximal order estimated for the system is 60 and the computational program used is according to that one developed by Schanke (2015).

The results of tests 1 and 2 from the SSI-COV method (Fig. 5a and 5b), showed that the poles stabilized at the natural frequencies corresponding to the three vibration modes identified, with magnitude of block rows $b=1$. For the same tests in the SSI-DATA method (Fig. 6a and 6b), $b=10$ was required to obtain better results. From this method it is possible to identify the natural frequencies, however there is a greater number of unstable and misaligned poles next to the physical poles of the three vibration modes. A possible reason is that these spurious poles appeared due to the high order value (number of block rows $b = 10$), as mentioned by Schanke (2015).

Considering the test 3 (Fig. 5c and 6c), stabilization occurred with a magnitude of $b=10$ for both methods and the diagrams obtained are similar. However, there are stable and aligned poles corresponding to other frequencies that do not correspond to the natural frequencies of the frame. The appearance of these poles may have been caused by the vibration of the electric motor used in the test. This motor was not isolated from the system. The dynamic action of the motor was not measured; however, it is known that its frequency was fixed and with a value nearly 7 Hz, that corresponding to the first natural frequency of the frame.

In order to distinguish the system's own frequencies, in Test 3, the values of the theoretical frequencies were taken into account, as well as the eigenvectors (modal forms) corresponding to the values identified in the stabilization diagram. The acquisition of the records during this test was done after the electric motor started, and before it stopped, disregarding, therefore, these two actions.

The Modal Assurance Criterion (MAC) (Allemang and Brown, 1982; Allemang, 2003; Miroslav Pastor *et al.*, 2012) measures the correlation between the experimental and the theoretical mode shapes. As result, a matrix is obtained and the values of the main diagonal indicate the correlation between the corresponding modes. The values vary between 0 and 1 and 1 indicates that there is a good agreement between the analyzed mode shapes. Fig. 7 presents a comparison between mode shapes identified by the Peak Picking Method (Fig. 7a), SSI-COV/ref (Fig. 7b) and SSI-DATA/ref (Fig. 7c) for all tests. Table 3 presents the values of the MAC diagonal obtained from the realized tests for all methods.

Table 3. MAC diagonal calculated between the experimental and theoretical modes.

Peak Picking Method			
Mode Shapes	Test 1	Test 2	Test 3
1^{st}	0.9995	0.9995	0.9992
2^{nd}	0.9990	0.9991	0.6608
3^{rd}	0.9966	0.9975	0.9998
SSI-COV/ref			
Mode Shapes	Test 1	Test 2	Test 3
1^{st}	0.9984	0.9985	0.9985
2^{nd}	0.9993	0.9986	0.9986
3^{rd}	0.9982	0.9987	0.9987
SSI-DATA/ref			
Mode Shapes	Test 1	Test 2	Test 3
1^{st}	0.9820	0.9813	0.9857
2^{nd}	0.9980	0.9973	0.9972
3^{rd}	0.9913	0.9876	0.9884

The Peak Picking Method has a satisfactory correlation between the experimental and theoretical modes, except for the second mode, as identified from Test 3 (Fig. 7a). This value indicates a correlation of 66.08% calculated from MAC index. For SSI-COV/ref it can be verified that a good agreement between the experimental and theoretical modes exists. For SSI-DATA/ref the mode shapes identification was more uniform than that observed for the other methods.

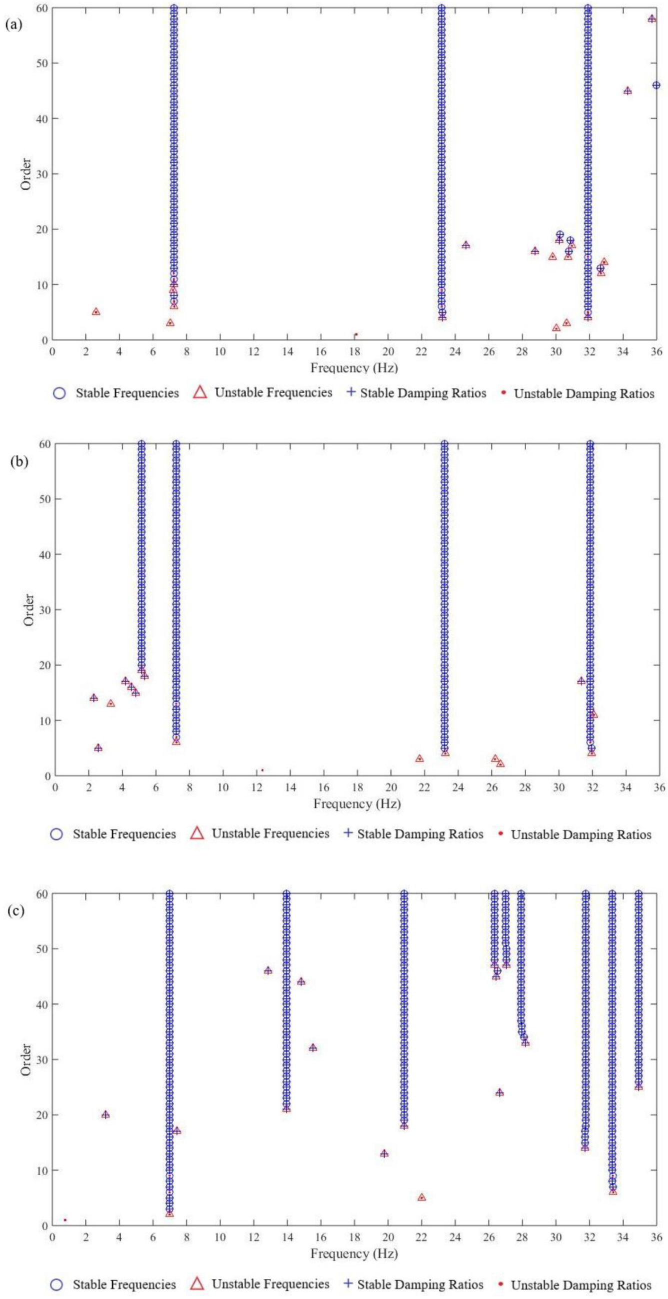

Fig. 5. Stabilization diagrams by SSI-COV method.

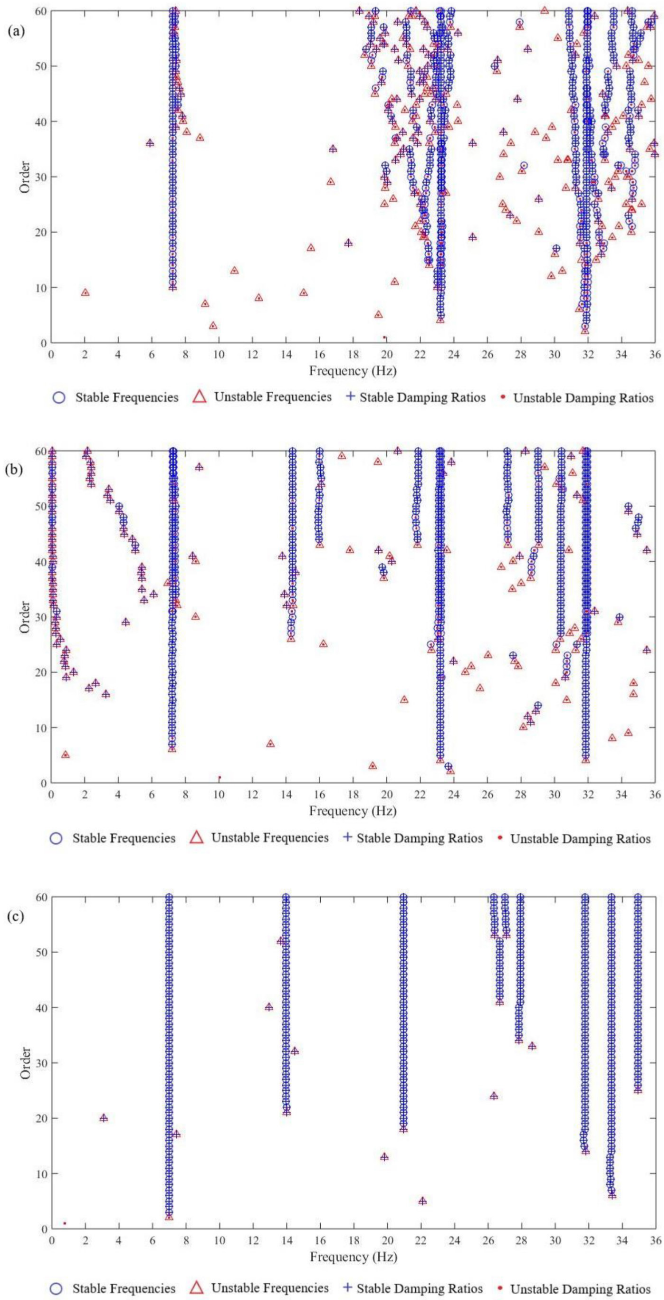

Fig. 6. Stabilization diagrams by SSI-DATA method.

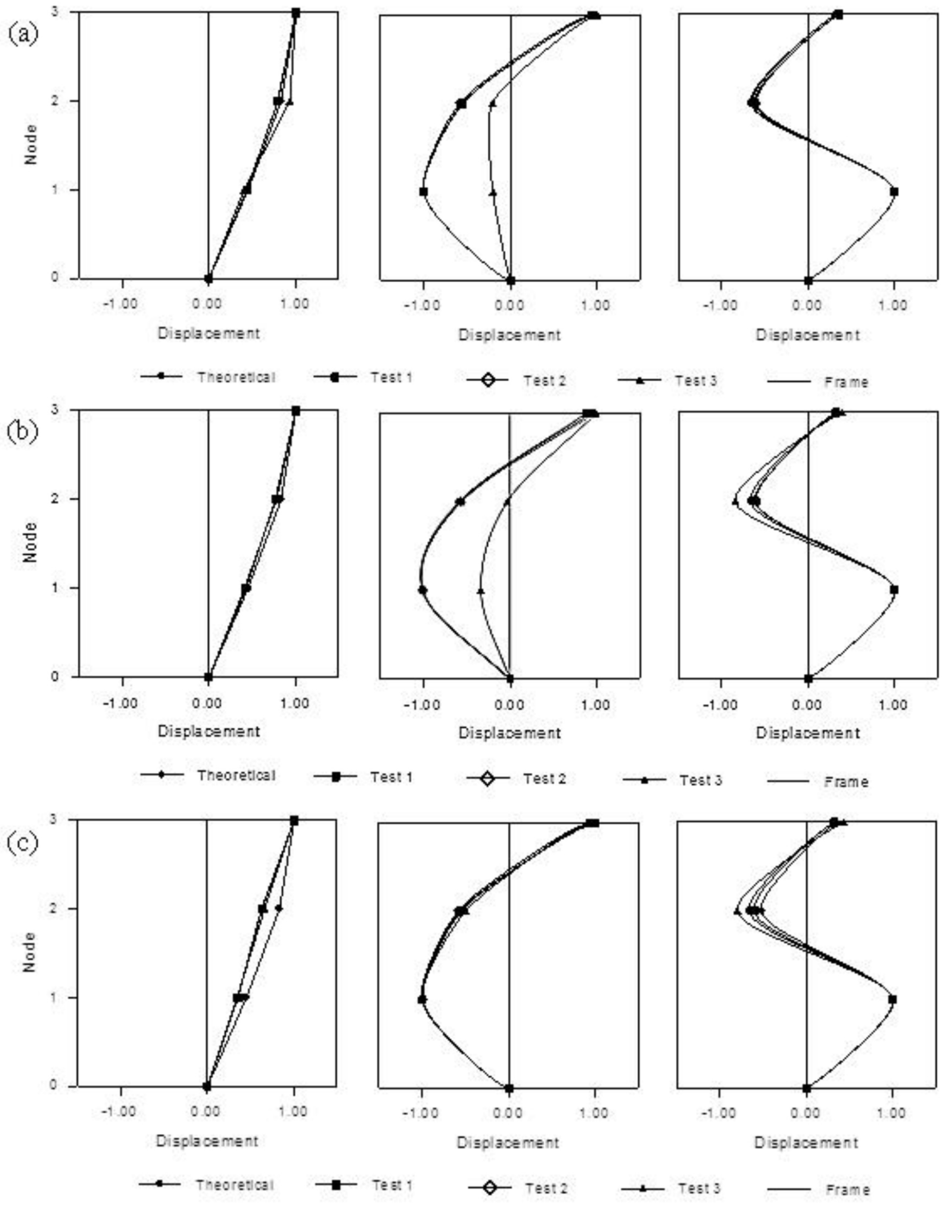

Fig. 7. Comparison between mode shapes identified by all methods for each realized test.

6.3 Frame finite element model updating

A numerical model of a structure can be very useful in the forecast of its behavior front to different configurations which can be produced by several load conditions or by modifications suffered along structure structure's life time. However, there are discrepancies between numerical predictions and experimental results, which may impose some restrictions for the use of this model. Updating the model is necessary in order to modify its parameters and improve the agreement or the correlation between the experimental and numerical results.

Although the experimental and numerical results have had a good approximation, the finite element model of the frame was updated in order to improve this approach much more. The update was made from the initial model shown in Fig. 8. The parameters K1, K2, K3, M1, M2 and M3 were updated and their initial values are summarized in Table 4. In this case, there were more parameters to be updated than measures (three natural frequencies), so the algorithm used was that defined by Eq. (16). It is important to note that in order to verify the confidence of the implemented algorithm, some simulations have been done and the results are presented in Brasiliano (2005).

The frame experimental frequencies, identified by SSI-DATA/ref, were used in the update process. The values presented in the second column of Table 4 represent the vector of parameters $\boldsymbol{\theta}_0$. The eigenvalues sensitivity matrix, $\mathbf{S} \in R^{3\times 6}$ was calculated according to Eq. (14). For calculating the weighting matrix $\mathbf{W}_{\varepsilon\varepsilon}$, a standard deviation of 0.25% was assumed for each experimental frequency. Thus, the standard deviation of the eigenvalues was approximately 0.50%.

Table 4. Model updating results.

Values of the parameters. Units: K (N/m) e M (Kg).							
	Initial Param.	Number of iterations					Updated Parameters
		3	10	19	28	35	
K1	4176.163	4217.984	4220.946	4220.971	4220.971	4220.971	4220.971
K2	3695.382	3623.679	3614.025	3613.947	3613.947	3613.947	3613.947
K3	3695.382	3687.678	3685.842	3685.828	3685.828	3685.828	3685.828
M1	0.350	0.326	0.327	0.327	0.327	0.327	0.327
M2	0.420	0.433	0.436	0.436	0.436	0.436	0.436
M3	0.268	0.226	0.225	0.225	0.225	0.225	0.225

Frequency values. Units: Frequency (Hz).								
	Freq. Initial Model	Number of iterations					Frequency of updated model	Exp. frequencies
		2	7	10	20	35		
1st	7.158	7.310	7.234	7.232	7.231	7.231	7.231	7.230
2nd	22.219	23.260	23.180	23.179	23.178	23.178	23.178	23.182
3rd	30.524	32.131	31.867	31.868	31.868	31.868	31.868	31.868

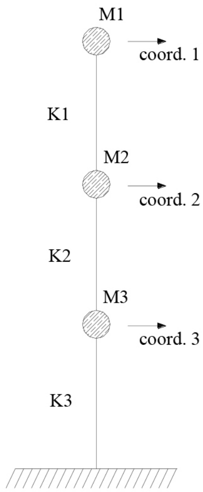

Fig. 8. Frame initial model.

For calculating $\mathbf{W}_{\theta\theta}$, a standard deviation of approximately 3% and 20% were assumed for each initial stiffness and mass, respectively. It is relevant to point out that the values in the weighting matrices represent the reciprocals of the variances (the squares of the standard deviations). The weighting matrices were as follows (Eq. 19):

$$\begin{aligned} \mathbf{W}_{\theta\theta} &= \mathrm{diag}\left[5.297\mathrm{x}10^{-5} \quad 6.765\mathrm{x}10^{-5} \quad 6.765\mathrm{x}10^{-5} \quad 2.040\mathrm{x}10^{2} \quad 1.420\mathrm{x}10^{2} \quad 3.488\mathrm{x}10^{2}\right] \\ \mathbf{W}_{\varepsilon\varepsilon} &= \mathrm{diag}\left[9.391\mathrm{x}10^{-3} \quad 8.886\mathrm{x}10^{-5} \quad 2.488\mathrm{x}10^{-5}\right] \end{aligned} \tag{19}$$

Table 4 presents the obtained results of the updating process for the parameters and frequencies of the updated model, respectively. Despite the inherent errors in the measured data and the possible differences between the initial and real models, it can be verified that the updated model (constructed with the updated parameters) can reproduce the experimental frequencies accurately. Although iterative methods yield updated parameters with physical meaning it is difficult to affirm if the parameters obtained correspond to those of the real structure, even so their values seem to be representative of the reality.

Fig. 9a and 9b present the convergence of the parameters and frequencies, respectively. These figures verify that a fast convergence, about the tenth iteration occurs.

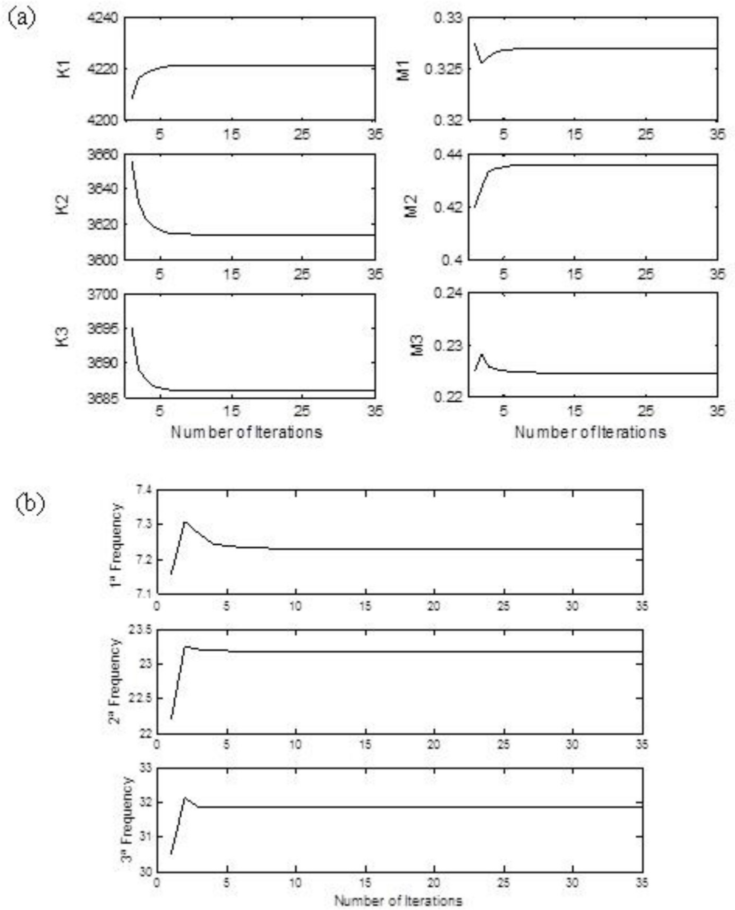

Fig. 9. Convergence of the updated parameters and frequencies.

7. Conclusions

About the free vibration tests (Tests 1 and 2), the Peak Picking Method, SSI-COV/ref and SSI-DATA/ref allowed the satisfactory identification of the three mode shapes of the structure. Small differences were observed, such as the displacement amplitude that, depending on the type of applied excitation, had a better matching with the theoretical ones.

Better results have been obtained for the first natural frequency considering all the applied methods. Compared with the theoretical frequencies, the values identified from the Peak Picking method presented a difference of 0.866%, and the other two methods yielded a difference of about 1%. For the second and third frequencies, the better results were obtained by the SSI-DATA/ref, except for the third frequency from Test 3.

Generally, the SSI-DATA/ref presented better results for the analyzed cases, since that even in the case of forced vibration test, the identification of second mode shape was less affected by the excitation induced by the motor. On the other hand, the Peak Picking and SSI-COV/ref presented a better processing velocity performance resulting in less computational effort.

Considering the model updating, the algorithm applied have presented a good performance in the parameters updating, which allowed matching the frequencies provided by the numerical model to those measured experimentally. A fast convergence could also be observed for the parameters and frequencies.

In order to establish a methodology for continuous monitoring structures the identification of modal properties and numerical model updating are necessary tools and some alternatives have been considered in this paper. Nevertheless, the results presented in this study could be complemented by a third step which would be the application of damage identification methods, based on the dynamic properties, considering the updated model and the natural frequencies and mode shapes identified by the output-only identification methods.

Acknowledgments

This research work was partly supported by Coordenação de Aperfeiçoamento de Pessoal de Nível Superior – CAPES and Conselho Nacional de Desenvolvimento Científico e Tecnológico – CNPq (Brazil). The authors are also grateful to the staff of the vibration laboratory of Department of Mechanical Engineering of the Brasilia University.

References

Allemang, R. J. (2003). The modal assurance criterion–twenty years of use and abuse. *Sound and Vibration*, *37*(8), 14–23.

Allemang, R. J., & Brown, D. L. (1982). A correlation coefficient for modal vector analysis. *In Proceedings of the 1st Int. Modal Analysis Conference*, Orlando, Florida, 8–10 November 1982.

Brasiliano, A. (2005). Identificação de Sistemas e Atualização de Modelos Numéricos com Vistas à Avaliação da Integridade Estrutural. PhD thesis, Faculdade de Tecnologia, Universidade de Brasília, Brasília, Brazil.

Brownjohn, J. M. W., Xia, P-Q, Hao, H., & Xia, Y. (2001). Civil Structure Condition Assessment by FE Model Updating: Methodology and Case Studies. *Finite Element and Analysis Design, 37*, 761–775.

Carone, C. (2018). Laudo da PCDF aponta que queda de viaduto poderia ter sido evitada. Metrópoles. Available from *https://www.metropoles.com/distrito-federal/laudo-da-pcdf-aponta-que-queda-de-viaduto-poderia-ter-sido-evitada* [accessed 9 August 2019].

Cerqueira, R. (2018). Problema em apoio pode ter provocado queda de viaduto em SP, diz especialista. Globo G1. Available from *https://g1.globo.com/sp/sao-paulo/noticia/2018/11/15/especialista-diz-que-problema-em-apoio-provocou-queda-de-viaduto-em-sp.ghtml* [accessed 9 August 2019].

Chen, Chi-Tsong. (1999). *Linear System Theory and Design*. Oxford University Press, N.Y.
Clough, R. W., & Penzien, J. (1993). *Dynamic of Structures*. Mc Graw-Hill, New York.
Doebling, S. W., Farrar, C. R., & Prime, M. B. (1998). A summary Review of Vibration-Based Damage Identification Methods. *The Shock and Vibration Digest*, *30*(2), 91–105.
Friswell, M., & Mottershead, J. E. (1995). *Finite Element Model Updating in Structural Dynamics*. Kluwer Academic Publishers Group, Dordrecht, Netherlands.
Fox, R. L., & Kapoor, M. P. (1968). Rate of Changes of Eigenvalues and Eigenvectors. *AIAA Journal*, *6*(12), 2426–2429.
Juang, Jer-Nan. (1994). *Applied System Identification*. Prentice Hall PTR, Upper Saddle River, N.J.
Pastor, M., Binda, M., & Harčarik, T. (2012). Modal assurance criterion. *Procedia Engineering, 48*, 543–548
Palazzo, G. L. (2001). Identificación del Daño Estructural a través del Cambio en las Propiedades Dinámicas. M.Sc. thesis, Instituto de Estructuras, Universidad Nacional de Tucumán, Argentina.
Peeters, B. 2000. System Identification and Damage Detection in Civil Engineering. PhD thesis, Departement Burgerlijke Bouwkunde, Katholieke Universiteit Leuven, Belgium.
Peeters, B., & De Roeck, G. (1999). Reference-Based Stochastic Subspace Identification for Output-Only Modal Analysis. *Mechanical Systems and Signal Processing, 13*(6), 855–878.
Peeters, B., & De Roeck, G. (2001). Stochastic System Identification for Operational Modal Analysis: A Review. *Journal of Dynamic Systems, Measurement, and Control, 123*, 659–667.
Rahman, M. S. (2012). Comparison of System Identification Techniques with Field Vibration Data for Structural Health Monitoring of Bridges. M.Sc. thesis, Faculty of Graduate Studies and Postdoctoral, Carleton University, Ottawa, Canada.
Schanke, A. S. (2015). Operational Modal Analysis of Large Bridges. M.Sc. thesis, Fakultet for Ingeniorvitenskap og Teknologi, Norges Teknisk-Naturvitenskapelige Universitet, Trondheim, Norway.
Welch, P. D. (1967). The Use of Fast Fourier Transform for the Estimation of Power Spectra: A Method Based of Time Averaging Over Short, Modified Periodograms. *IEEE Transactions on Audio and Electroacoustics, 15*, 70–73.
Zou, Y., Tong, L., & Steven, G. P. (2000). Vibraton-Based Model-Dependent Damage (Delamination) Identification and Health Monitoring for Composite Structures – A Review. *Journal of Sound and Vibration, 230*(2), 357–378.

Andrea Brasiliano
Ingeniera Civil (Universidad Federal de Paraíba - UFPB - 1998), Máster (2001) y Doctorado (2005) en Estructuras y Construcción Civil (Universidad de Brasilia). Es profesora asociada en el Departamento de Ingeniería Civil y Ambiental, en UFPB desde 2009. Tiene experiencia en el campo de la Ingeniería Civil, con énfasis en Dinámica Estructural, trabajando en los siguientes temas: características dinámicas, estructuras, identificación de sistemas, integridad estructural y análisis experimental.

andrea.brasiliano@academico.ufpb.br

Maria Diciá D. Silva
Ingeniera Civil (Universidad Federal de Paraíba – 2018). Actuó en el “Programa de Monitoreo para las disciplinas del Departamento de Ingeniería Civil y Ambiental de la UFPB” (2017), investigación desarrollada en el área de identificación de propiedades dinámicas en estructuras reticuladas mediante análisis numérico y experimental en el Laboratorio de Ensayos de Materiales y Estructuras (LABEME/UFPB) (2018).

maria_dicia@hotmail.com

Graciela N. Doz
Doctora en Ingeniería (Universidad Nacional de Tucumán, Argentina 1995). Actualmente es profesora asociada en la Universidad de Brasilia (UnB). Publicó artículos en revistas especializadas y más de 100 obras en anales de congresos. También fue Directora de Proyectos en el Rectorado de la UnB y Coordinadora del Programa de Posgrado en Estructuras y Construcción Civil. Trabaja en el campo de la dinámica estructural, en particular en vibraciones inducidas en estructuras, control de vibraciones, evaluación de la integridad estructural y procesos de ruptura.

graciela@unb.br

José Luís Vital de Brito
Ingeniero Civil Universidad Estadual Paulista - 1974), Master en Ingeniería Civil (1979) y Doctor en Ingeniería Civil (Universidad Federal de Rio Grande do Sul-1995). Actualmente es profesor asociado en la Universidad de Brasilia. Actúa principalmente en estructuras, aerodinámica, efecto del viento en las estructuras, control de vibraciones e inestabilidad dinámica. Publica continuamente artículos en revistas indexadas y en congresos. Es también revisor de artículos para revistas nacionales e internacionales.

jlbrito@unb.br